



저작자표시-비영리-변경금지 2.0 대한민국

이용자는 아래의 조건을 따르는 경우에 한하여 자유롭게

- 이 저작물을 복제, 배포, 전송, 전시, 공연 및 방송할 수 있습니다.

다음과 같은 조건을 따라야 합니다:



저작자표시. 귀하는 원저작자를 표시하여야 합니다.



비영리. 귀하는 이 저작물을 영리 목적으로 이용할 수 없습니다.



변경금지. 귀하는 이 저작물을 개작, 변형 또는 가공할 수 없습니다.

- 귀하는, 이 저작물의 재이용이나 배포의 경우, 이 저작물에 적용된 이용허락조건을 명확하게 나타내어야 합니다.
- 저작권자로부터 별도의 허가를 받으면 이러한 조건들은 적용되지 않습니다.

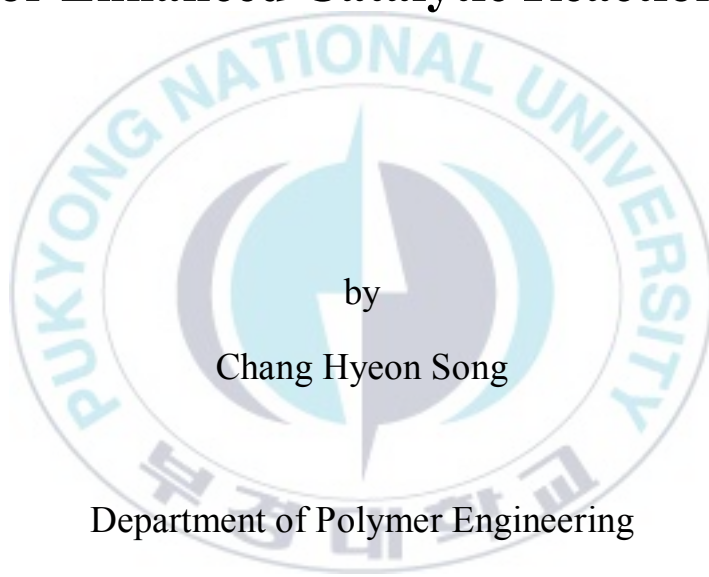
저작권법에 따른 이용자의 권리는 위의 내용에 의하여 영향을 받지 않습니다.

이것은 [이용허락규약\(Legal Code\)](#)을 이해하기 쉽게 요약한 것입니다.

[Disclaimer](#)

Thesis for the Degree of Master of Engineering

**Polymer-Nanoparticle
Composite Membranes
for Enhanced Catalytic Reactions**



by

Chang Hyeon Song

Department of Polymer Engineering

The Graduate School

Pukyong National University

August 2019

Polymer-Nanoparticle Composite Membranes for Enhanced Catalytic Reactions

Advisor: Prof. Seong Il Yoo

by

Chang Hyeon Song

A thesis submitted in partial fulfillment of the requirements
for the degree of

Master of Engineering

in Department of Polymer Engineering, The Graduate School,

Pukyong National University

Busan, South Korea

August 2019

Polymer-Nanoparticle Composite Membranes for Enhanced Catalytic Reactions

A thesis

by

Chang Hyeon Song

Approved by:

Prof. Joo Hyun Kim

Prof. Mun Ho Kim

Prof. Seong Il Yoo

August 2019

CONTENTS

| | |
|---|-----------|
| Contents | I |
| List of Tables | IV |
| List of Figures | V |
| Abstract..... | IX |
| Chapter I. Introduction | 1 |
| I-1. Polymer membranes | 1 |
| I-1.1. Selective Separation | 1 |
| I-1.2. Light Scattering | 3 |
| I-2. TiO ₂ Nanoparticles | 5 |
| I-2.1. Photocatalysis | 5 |
| I-2.2. Water Treatment | 7 |
| I-3. Gold Nanoparticles | 7 |
| I-3.1. Localized Surface Plasmon Resonance | 8 |
| I-3.2. Photothermal Effects | 10 |
| Chapter II. Enhanced Photocatalytic Activity of Immobilized TiO₂ Nanoparticles in PES Composite Membranes by Scattering-Mediated Absorption | 12 |

| | |
|--|---------------|
| II-1. Introduction | 12 |
| II-2. Experimental Section | 15 |
| II-2.1. Material | 15 |
| II-2.2. Procedure | 15 |
| II-2.2.1. Synthesis of TiO ₂ Nanoparticles | 15 |
| II-2.2.2. Synthesis of the PES/[PAH/PSS] ₂ /TiO ₂ Composite Membrane | 16 |
| II-2.2.3. Evaluation of Photocatalytic Activity | 16 |
| II-2.3. Measurement | 17 |
| II-3. Result and Discussion | 17 |
| II-3.1. Synthesis and Optical Properties of Dispersed TiO ₂ Nanoparticles | 17 |
| II-3.2. Synthesis and Structural Properties of PES/[PAH/PSS] ₂ /TiO ₂ Composite Membranes | 20 |
| II-3.3. Enhanced Photocatalytic Activity of Immobilized TiO ₂ Nanoparticles | 23 |
| II-3.4. Scattering-Mediated Absorption of PES/TiO ₂ Composite Membranes | 29 |
| II-4. Conclusion..... | 32 |
| Chapter III. Enhanced Photothermal Heating of Au Nanoparticles by Multiple Scattering Process in Composite Membranes for Heterogeneous Catalytic Reaction | 33 |

| | |
|---|----|
| III-1. Introduction | 33 |
| III-2. Experimental Section..... | 37 |
| III-2.1. Material | 37 |
| III-2.2. Procedure | 37 |
| III-2.2.1. Synthesis of Colloidal Au | 37 |
| III-2.2.2. Synthesis of the PES/[PAH/PSS] _{1.5} /Au Composite Membrane | 37 |
| III-2.2.3. Evaluation of Catalytic Reaction | 38 |
| III-2.3. Measurement | 38 |
| III-3. Result and Discussion..... | 39 |
| III-3.1. Synthesis and Structural Properties of the Composite Membranes | 39 |
| III-3.2. Catalytic Performance of the Composite Membrane | 44 |
| III-3.3. Evaluation of Local Temperature by the Composite Membrane | 48 |
| III-3.4. Combination of Multiple Scattering Process and Broadband Absorption..... | 51 |
| III-4. Conclusion | 54 |
| References | 55 |
| Acknowledgment..... | 60 |

LIST OF TABLES

- Table 1. The reaction rates of 4-NP by PES/Au composite membranes were repeated three times independently for each trial.



LIST OF FIGURES

- Figure 1. Schematic diagram of selective separation by polymer membranes.
- Figure 2. Schematic illustration of light-scattering by pores of polymer membranes.
- Figure 3. Schematic illustration of photocatalytic properties by TiO_2 . TiO_2 has the photocatalytic properties to generate radical species such as a hydroxyl radical and a superoxide anion radical after interacting with water and oxygen by receiving UV light.
- Figure 4. Schematic diagram of a localized surface plasmon resonance (LSPR) induced by an external electrical field.
- Figure 5. Schematic diagram of photothermal effects by Au NPs with illumination. It causes temperature increase in colloidal state.
- Figure 6. HR-TEM images (a) and UV-Vis spectrum (b) of TiO_2 NPs. The lattice structures of each TiO_2 NPs are marked by dashed circles in the HR-TEM image.
- Figure 7. (a – c) Plan-view and (d – e) cross-sectional SEM images of PES membranes with $[\text{PAH/PSS}]_2/\text{TiO}_2$ NPs with different magnifications.
- Figure 8. (a, b) Time-dependent UV-Vis spectra of photocatalytic decomposition of MB in the presence of PES/ TiO_2 composite membrane without (a) and with (b) light illumination. (c) Time-

dependent absorbance values at 664 nm in the time course of photocatalytic decomposition of MB with (red color) and without (blue color) light illumination. (d) TGA results of PES (black), PES/[PAH/PSS]₂ (blue), and PES/[PAH/PSS]₂/TiO₂ NPs under air environment.

Figure 9. (a, b) Time-dependent UV-Vis spectra of MB photocatalytic decomposition in the presence of colloidal TiO₂ NPs with (a) and without (b) light illumination. (c) Time-dependent absorbance values at 664 nm in the time course of MB photocatalytic decomposition with (blue color) and without (blue color) light illumination. (d) Comparison of kinetics of MB decomposition from dispersed TiO₂ NPs (blue color) and immobilized TiO₂ NPs (red color).

Figure 10. Diffuse reflectance of PES (blue) and PES/[PAH/PSS]₂/TiO₂ (red) membranes.

Figure 11. Graphical abstract of immobilized Au NPs on the PES membrane surface, the composite membrane. In the formed composite membrane, Au NPs generate heat with illumination, and a polymer membrane scatters the incident light to the outside or inside. The internally scattered light induces multiple scattering process, which is absorbed by Au NPs or re-scattered by the surface of the assembly.

Figure 12. (a) Time-dependent of extinction spectra of Au NPs after the immersion of PES membrane. (b) Reflectance spectra of PES (red line) and PES/Au membranes (blue).

Figure 13. Plane-view (a, b) and cross-sectional (c, d) FE-SEM images of PES/Au composite membranes under different magnifications.

Figure 14. (a, b) Time-dependent UV-Vis spectra of catalytic reaction of 4-NP in the presence of the PES/Au composite membrane under dark condition (a) and under light illumination (b). (c) Time-dependent absorbance values at 400 nm in the time course of 4-NP catalytic reaction under dark condition (blue line) and under light illumination (red line).

Figure 15. (a, b) Time-dependent UV-Vis spectra of catalytic reaction of 4-NP in the presence of PES/Au composite membranes at four different temperature conditions. (a) Time-dependent absorbance values at 400 nm in the time course of 4-NP catalytic reaction under 23.1 °C (black line), 30.6 °C (red line), 39.5 °C (blue line) and 51.8 °C (green line), respectively. (b) $\ln k$ versus $1/T$ of the straight line. The activation energy (E_a) can be calculated through its slope ($-\frac{E_a}{R}$).

Figure 16. (a) Time-dependent temperature measurement in the 4-NP catalytic experiment of the PES/Au composite membrane under dark container (blue line) or light illumination (red line). Images of the reactor taken with a thermal imaging camera after 360 min of

catalytic experiments start under light illumination (b) and dark container (c). (d) Irradiance spectra of the solar simulator (green line), absorption spectra of colloidal Au (red line) and the PES/Au composite membrane (blue line).



Polymer-Nanoparticle Composite Membranes for Enhanced Catalytic Reactions

Chang Hyeon Song

Department of Polymer Engineering,

The Graduate School

Pukyong National University

Abstract

Nanoparticles having catalytic properties are characterized in that they receive the light of a specific wavelength band and change the reaction rate by reducing the activation energy required for the chemical reaction. In general, to improve the catalytic properties of nanoparticles, researches have been actively conducted to form nanocomposites capable of responding to the light of a broader wavelength band by introducing heterogeneous nanoparticles. On the other hand, in this study, we carried out a study to amplify the catalytic reaction of nanoparticles using the scattering property of the polymer membrane. For this purpose, a composite membrane was prepared by immobilizing titanium dioxide nanoparticles or gold nanoparticles on a polyethersulfone (PES) polymer membrane, and the optical properties and the catalytic reaction of the composite membrane were evaluated depending on whether light was irradiated.

고분자-나노입자 복합체 멤브레인을 활용한 촉매 반응 증폭에 대한 연구

요약

촉매 특성을 가지는 나노 입자는 특정한 파장대의 빛을 받아 화학 반응에 필요한 활성화 에너지를 적게 만들어 반응속도를 변화시키는 특성을 가진다. 일반적으로, 나노 입자의 촉매 특성을 향상시키기 위해 이종의 나노 입자를 도입함으로써 더 넓은 파장대의 빛에 감응할 수 있는 나노 복합체를 형성하는 연구가 활발히 진행됐다. 이에 반해, 본 연구에서는 고분자 멤브레인의 산란 특성을 활용하여 나노 입자의 촉매 반응을 증폭하는 연구를 진행하였다. 이를 위해, 다기공성의 polyethersulfone (PES) 고분자 멤브레인에 이산화타이타늄 나노입자 혹은 금 나노입자를 고정화하여 복합체 멤브레인을 형성하고, 형성된 복합체 멤브레인의 광학 특성 및 촉매 반응을 광 조사 유무에 따라 평가하였다.

Chapter I. Introduction

I-1. Polymer Membranes

The membrane is a selective barrier that is located between two systems of fluids, which exchange energy and material. A membrane has applied a concentrated resistance to the moving fluid which selectively effects on the material so that separation of the two phases occurs due to the difference in the flow rate. Membranes can be classified into various types according to their material properties, structures, applications and roles of membranes. A membrane consisting of macromolecules is called a polymer membrane.

I-1.1. Selective Separation

The polymer membranes are mainly handled in the process of removing undesirable chemicals, biological contaminants, suspended solids, and gases [1-3]. In this process, one of the most important functions of polymer membranes is selective separation. The common application of selective separation is oil-water separation [1,4]. Selective separation has been achieved by controlling the degree of hydrophilicity of the polymer membranes surface itself. In addition, studies have been made to increase the efficiency of separation of polymer membranes by applying other hydrophilic materials [5-7].

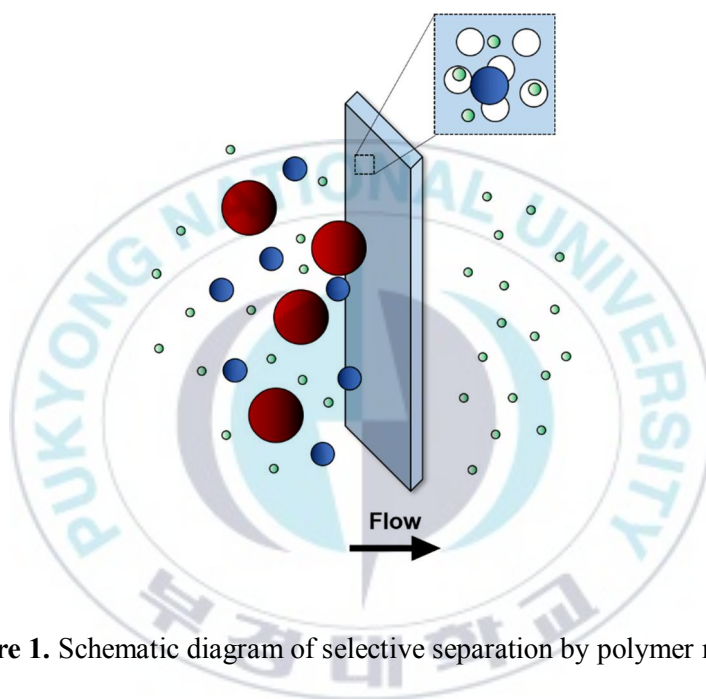


Figure 1. Schematic diagram of selective separation by polymer membranes.

I-1.2. Light Scattering

When directly observing light scattering, the substance causing light scattering appears opaque [8]. For example, a relatively high concentration of a polymer solution is not transparent. It means that the polymer solution can interact with the light-sensitive material. Moreover, a variety of polymer-nanoparticle nanocomposites such as polymer-encapsulated metal nanoparticles have been passionately studied [9-10]. In this study, we aimed to utilize the light-scattering property of polymer membranes rather than polymers in solution. The polymer membranes are basically opaque or semitransparent because it has a rough surface and a lot of pores that causes light-scattering. The scattered light within the polymer membrane would be re-scattered between different surfaces in the membrane, which was expected to play an excellent role in increasing the efficiency of photo-sensitive nanoparticles (NPs). In order to demonstrate this expectation, the catalytic properties of polymer-nanoparticle composite membranes by immobilizing TiO₂ NPs or Au NPs were evaluated using polyethersulfone (PES) membranes.

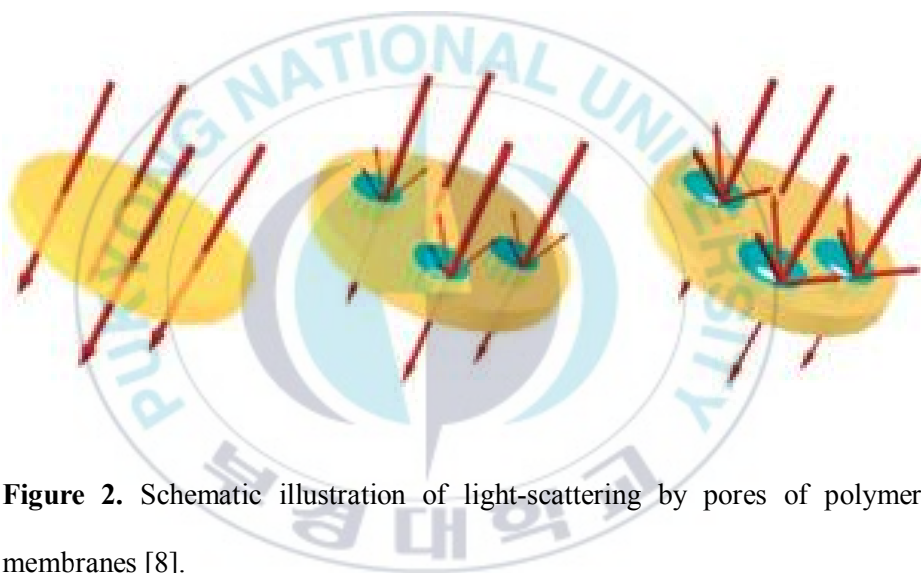


Figure 2. Schematic illustration of light-scattering by pores of polymer membranes [8].

I-2. TiO₂ Nanoparticles

Titanium dioxide nanoparticles (NPs), also called ultrafine titanium dioxide or nanocrystalline titanium dioxide or microcrystalline titanium dioxide, are particles of titanium dioxide (TiO₂) with diameters less than 100 nm. TiO₂ is used in UV protection cosmetics due to its capability to block ultraviolet (UV) light. In recent decades, water treatment systems utilizing the photocatalytic properties of TiO₂ NPs have been extensively studied [11-12].

I-2.1. Photocatalysis

TiO₂ NPs have the photocatalytic properties that interact with water to absorb UV light having higher energy than their band gap to generate holes and electrons. As the resulting hole and electrons, hydroxyl radicals and superoxide radical anions are generated, respectively. In general, these radical species are known to decompose organic pollutants and have the antimicrobial activity [11-13]. In this study, enhanced photocatalytic effect was confirmed using methylene blue decomposition, which is a representative model of organic pollutants in order to evaluate the photocatalytic effect of the polymer-TiO₂ NPs composite membranes [14].

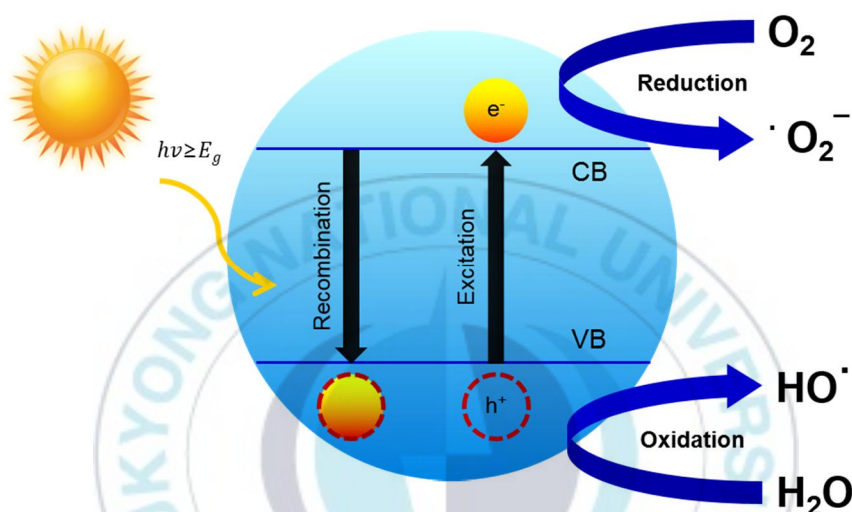


Figure 3. Schematic illustration of photocatalytic properties by TiO₂. TiO₂ has the photocatalytic properties to generate radical species such as a hydroxyl radical and a superoxide anion radical after interacting with water and oxygen by receiving UV light [11-13].

I-2.2. Water Treatment

Recently, numerous water treatment technologies, such as precipitation, antibiological treatment, appropriate oxidation techniques, have been evaluated to solve the worsening problem of clean water shortages. Moreover, water shortages are becoming key issues following rapidly increasing industry scale, the environmental contaminant and unpredictable climate changes. Therefore, a variety of water treatment systems have been developed to address these global water shortages [15]. However, there are few cost-effective and energy-efficient treatment methods for hazardous removal. Because of the price competitiveness, stability, wide specific surface area and non-toxicity, which are typical advantages of TiO_2 NPs, it has been confirmed that the water treatment system using TiO_2 NPs can be an alternative with great potential [11-12,15]. Basically, research has been carried out to utilize the photocatalytic effect according to the shape and size of TiO_2 NPs [16-17]. In addition, various studies have been made to improve the photocatalytic efficiency by doped TiO_2 NPs with other materials [18-19]. In this study, we tried to enhance the photocatalytic properties of TiO_2 NPs by using light scattering, one of the characteristics of polymer membranes.

I-3. Gold Nanoparticles

Gold is a chemical element with symbol Au and its atomic number 79. It is called

gold nanoparticles (Au NPs) that are made of particles with a diameter of about 1 to 100 nm by synthesis or assemblies. Like other nanoparticles, Au NPs also have a very large specific surface area. Moreover, such a large specific area has excellent advantages over the bulk state in chemical reactions. For example, there is a catalytic reaction of the 4-nitrophenol that proceeds on the surface of Au NPs. For decades, studies have been actively carried out to enhance the properties of Au NPs, which are photothermal effect and surface enhanced Raman scattering (SERS), by combining various other materials [9,20]. In this study, we utilized photothermal effect of Au NPs to immobilize them on polymer membranes, which have light scattering properties, and evaluate their enhanced catalytic properties.

I-3.1. Localized Surface Plasmon Resonance

The Plasmon is defined as a quantum of plasma oscillation. When the electric field of the visible-near infrared light is matched with plasmons of metal nanoparticles, the absorption of the incident light occurs, which causes the specific colors to appear. This phenomenon in metal nanoparticles is called localized surface plasmon resonance (LSPR), which locally generates the highly increased electric field. The interaction of metal nanoparticles with incident light has recently attracted attention in the field of nanotechnology [21].

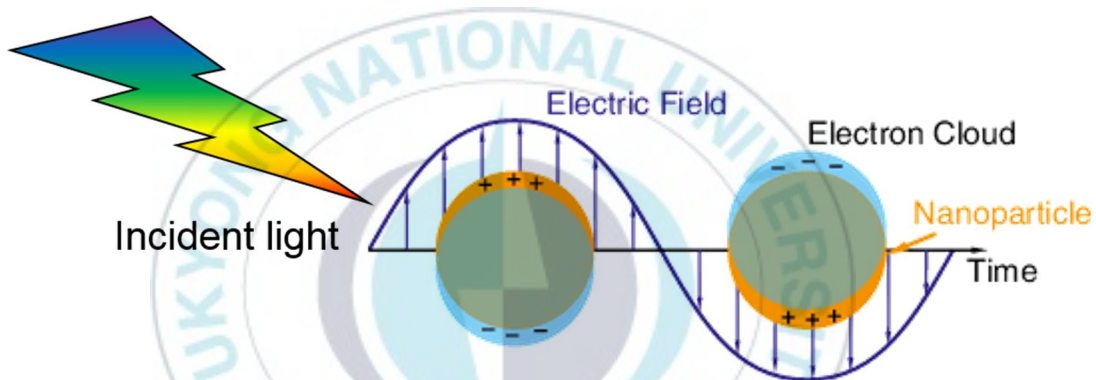
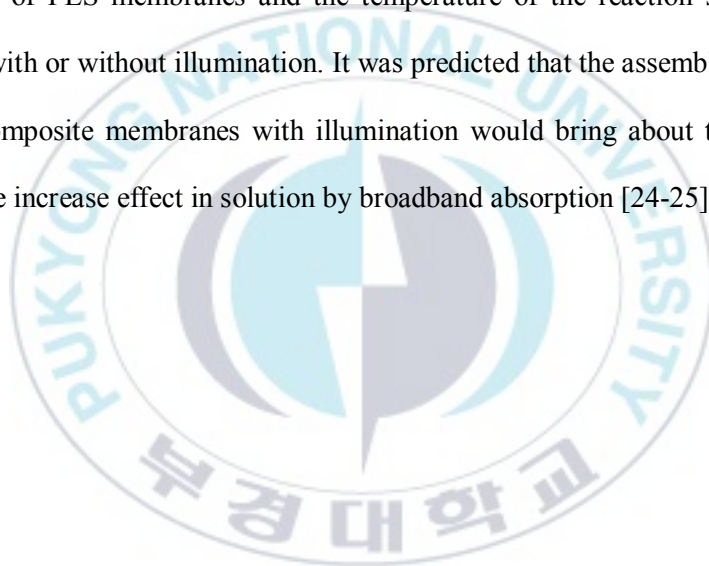


Figure 4. Schematic diagram of a localized surface plasmon resonance (LSPR) induced by an external electrical field.

I-3.2. Photothermal Effects

Au NPs have photothermal properties that generate heat by receiving electromagnetic waves of about 520 nm. For a couple of decades, studies applying Au NPs to photothermal therapy (PPTT) have been actively published in field of biotherapy [22]. Basically, Au NPs are utilized to eliminate the cancer cells in an organism by utilizing the heat generated [22-23]. In this paper, Au NPs were electrostatically adsorbed onto the surface of PES membranes and the temperature of the reaction solution was measured with or without illumination. It was predicted that the assembled polymer-Au NPs composite membranes with illumination would bring about the excellent temperature increase effect in solution by broadband absorption [24-25].



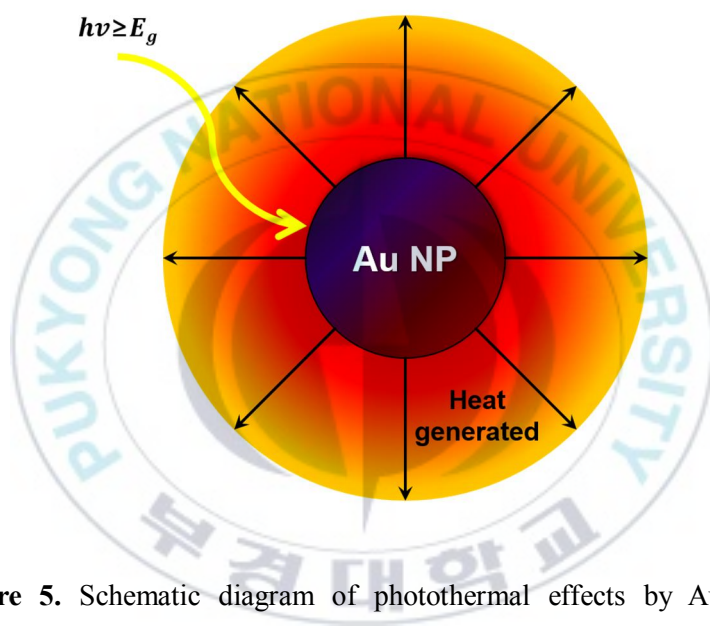


Figure 5. Schematic diagram of photothermal effects by Au NPs with illumination. It causes temperature increase in colloidal state.

Chapter II. Enhanced Photocatalytic Activity of Immobilized TiO₂ Nanoparticles in PES Composite Membranes by Scattering-Mediated Absorption

* This chapter is under review at *Polymer Composites*.

II-1. Introduction

Compared with a conventional water purification process based on chemical treatments, the application of photocatalytic nanoparticles (NPs) for the water purification has received a great deal of attentions because photocatalytic NPs can decompose organic contaminants without the production of harmful byproducts [12,26-27]. In general, semiconductor NPs can be photo-excited by UV source having higher energy than their band gap and generate electrons and holes to initiate redox reaction with H₂O and O₂ molecules at the NP surface. As a result, reactive oxygen species such as hydroxyl radicals ($\cdot\text{OH}$) and superoxide anion radicals ($\cdot\text{O}_2^-$) are produced, which can decompose organic pollutants into non-toxic materials and exert antimicrobial effects on numerous bacteria and virus [12,26-27]. While many inorganic NPs can be potentially useful for the water treatment, TiO₂ NPs have been extensively studied in the past owing to their easy synthesis, commercial availability,

stability, and low toxicity [12,26,28-31]. In particular, since the photocatalytic reaction is initiated at the NP surface, dispersed TiO₂ NPs in an aqueous suspension have been the focus of the early investigation because they can provide the largest surface area [2,28-31].

However, from practical point of view, the dispersed NPs have a number of problems because they must be separated from the purified suspension after photocatalytic reaction, which necessitates additional energy and cost [12,26-27]. In addition, the dispersed NPs can be easily aggregated in the contaminated water; this substantially reduces their catalytic activity. To overcome these issues, TiO₂ NPs have been immobilized into solid supports [5,14,33-39]. In particular, water filtration membranes in forms of porous polymers have been widely employed because the resulting composite membranes with photocatalytic function could provide not only an appropriate NP immobilization but also a mean to reduce fouling problem in membrane filtration [5,14,36-39]. As well understood, membrane filtration is the primary method for water treatment, but has been suffering from fouling due to the deposition of numerous contaminants and micro-organism in the feed stream [15,40]. In this regard, the introduction of photocatalytic activity inside the porous membranes can effectively decompose the deposited contaminants. In addition, the presence of TiO₂ NPs can increase the surface hydrophilicity of polymer membranes. Collectively, composite membranes with TiO₂ NPs exhibited improvement in decomposition of contaminants, permeate flux, and fouling resistance, in comparison with neat membrane [5,14,36-39].

Despite the large number of publications on the positive NP effects on the membrane filtration, however, there has been little clarity on the photocatalytic efficiency of the immobilized NPs. At first glance, it can be expected that the immobilized NPs would substantially lose their catalytic function because (a) the NP surface would be deactivated after being absorbed to the membrane wall, and (b) both reactants and products must diffuse in and out through the porous membranes, reducing the rate of reaction. On the contrary to this common anticipation, in this study, we attempt to explore an alternatively possibility that the presence of polymer membranes can promote the photocatalytic activity of the immobilized NPs. Although this opportunity has not been previously discussed in the literature, one can reach to this anticipation by considering the light scattering property of polymer membrane. As well known, the white and opaque appearance of typical polymer membranes are generated by high degree of light scattering and reflection at the interfaces of randomly oriented porous structures [8]. In this sense, the immobilized NPs in the membrane surface would be photo-excited by not only the external light source, but also the scattered light within the membrane. As a result, the actual number of photons that can be absorbed by immobilized NPs would be enormously increased by the multiple scattering events to enhance the photo-catalytic activity.

From this perspective, we questioned whether the polymer membranes could behave as inhibitor or promoter in photocatalytic reaction. To address this question, we synthesized and incorporated TiO₂ NPs into polyethersulfone membrane by layer-by-layer method. The photocatalytic activity of the prepared composite membranes was

tested against decomposition reaction of dye molecules. By comparing the reaction kinetics, we found the photocatalytic activity of immobilized TiO₂ NPs was higher than that of dispersed NPs in a solution state. The underlying mechanism of the unexpected catalytic function of immobilized NPs can be attributed to scattering-mediated absorption process in the composite membranes, which has been further supported by the optical properties of composite membranes.

II-2. Experimental Section

II-2.1. Material

Polyethersulfone (PES) filtration membranes (diameter: 25 mm, pore size: 450 nm) were provided by Scilab Co., Korea. Poly(allylamine hydrochloride) (PAH, weight-average molecular weight = 17,500 g/mol), poly (sodium 4-styrenesulfonate) (PSS, 70,000 g/mol), titanium (IV) isopropoxide (TTIP) and methylene blue (MB, ≥82 %) were obtained from Sigma-Aldrich. Ethyl alcohol (99.9%) was purchased from Duksan Co., Korea. Nitric acid (60%) was procured from Junsei Chemical Co., Japan. All the chemicals were used as received.

II-2.2. Procedure

II-2.2.1. Synthesis of TiO₂ Nanoparticles

Colloidal TiO₂ NPs were synthesized by the sol-gel process of precursor TTIP

according to a literature [32]. In brief, 1.25 mL of TTIP was added to 25 mL of ethyl alcohol, which was instilled into 250 mL of aqueous nitric acid solution at pH 1.5. The mixture was vigorously stirred for overnight. To obtain TiO₂ NPs in a powdery state, the solvent of the resulting NP solution was evaporated using a rotary evaporator at 40 °C.

II-2.2.2. Synthesis of the PES/[PAH/PSS]₂/TiO₂ Composite Membrane

To construct layer-by-layer (LbL) assemblies, 1.0 wt% aqueous solutions of positively-charged PAH and negatively-charged PSS were prepared. Since PES membrane has negative surface charge, the membrane was first immersed in an aqueous PAH solution for 3 h to deposit positively-charged PAH [36,41]. Subsequently, PAH-coated PES membrane was alternatively immersed in an aqueous solution of negatively-charged PSS for 3hr, which produced PAH/PSS bilayer on the PES membrane. In between each coating step of PAH (or PSS) layer, the membrane was immersed in deionized water for 1 hr to remove physisorbed PAH (or PSS) polymers. The coating process continued to produce a multi-layered film consisting of two bilayer of [PAH/PSS] on PES membrane, the structure of which will be denoted as PES/[PAH/PSS]₂. The chemically modified PES membrane was immersed in the aqueous solution of TiO₂ NPs for 1 week. Finally, the composite PES/[PAH/PSS]₂/TiO₂ membrane was immersed in deionized water for 3 h and further treated with ultrasonication for 5 min to remove physisorbed TiO₂ NPs.

II-2.2.3. Evaluation of Photocatalytic Activity

For the photocatalytic reaction, either TiO₂ NPs or PES/[PAH/PSS]₂/TiO₂ membrane were added into an aqueous solution of methylene blue (15 mL, 6 μM). The reaction mixture was placed either in dark container or illuminated by solar simulator. At a regular time interval, an aliquot of reaction mixture was taken to measure UV-Vis spectra. After measurement, the measured solution was poured back into the reaction mixture.

II-2.3. Measurement

UV-Vis spectra were obtained using an Agilent Technologies Cary 8454 UV-Vis spectrophotometer. A high-resolution transmission electron micrograph (HR-TEM) was recorded by a JEOL JEM-2100F microscope, working with a 200 kV accelerating voltage. Field-emission scanning electron microscopy (FE-SEM) images were taken with a Hitachi High-Technologies S-4800. Thermogravimetric analysis was made using a Perkin-Elmer TGA-7. The photocatalytic experiments were performed under simulated solar light irradiation working with 1.0 sun at AM 1.5 G, using an Abet Technologies LS-150 equipped with an infrared cut-off filter. Diffuse reflectance of the membranes was recorded on a Shimadzu SolidSpec-3700 UV-Vis-NIR spectrophotometer.

II-3. Result and Discussion

II-3.1. Synthesis and Optical Properties of Dispersed TiO₂ Nanoparticles

Before examining catalytic activity of the immobilized TiO₂ NPs in polymer membranes, we first synthesized TiO₂ NPs by hydrolysis of titanium(IV) isopropoxide, and dispersed them in deionized water to yield a 0.5 g/L solution. The pH value of the NP solution was about 2.8. In this pH value, TiO₂ NPs had a positively-charged surface with a zeta-potential value of ca. + 45 mV, which can be attributed to the protonation of hydroxylated TiO₂ surface as -TiOH₂⁺ [27]. As shown in the HR-TEM image (Figure 6a), the synthesized TiO₂ NPs has an average diameter of about 4 - 5 nm, which was quite comparable with the diameter obtained by dynamic light scattering (ca. 4.6 nm). Owing to the relatively small diameter, the onset of absorption of TiO₂ NPs was more or less blue-shifted from bulk value (387nm) and placed at 335 nm as in Figure 6b.

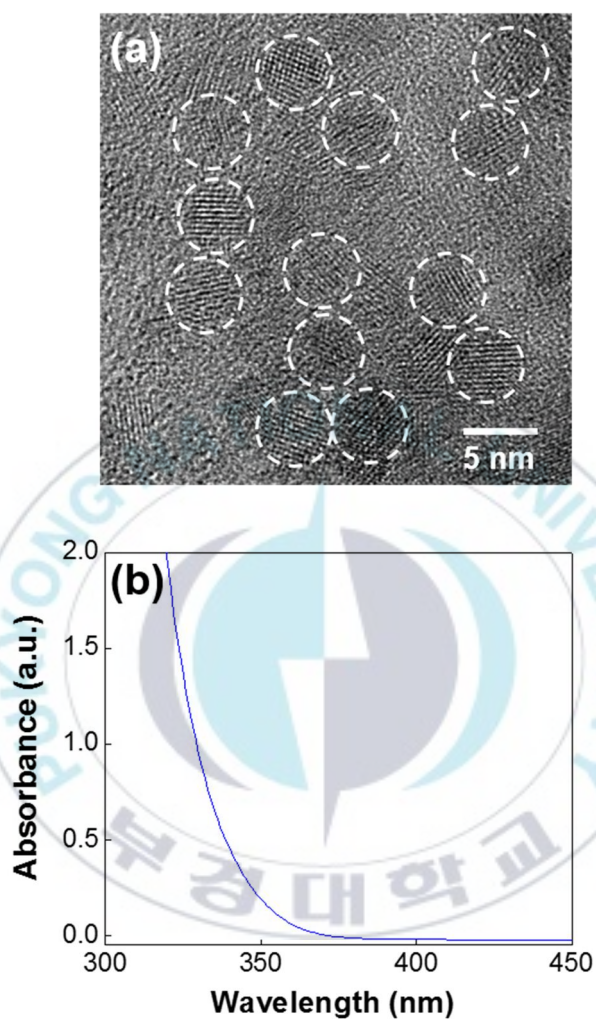


Figure 6. HR-TEM images (a) and UV-Vis spectrum (b) of TiO₂ NPs. The lattice structures of each TiO₂ NPs are marked by dashed circles in the HR-TEM image.

II-3.2. Synthesis and Structural Properties of PES/[PAH/PSS]₂/TiO₂ Composite Membranes

As a counterpart of TiO₂ NPs, we selected commercially available PES membranes because of their mechanical, thermal, and chemical stability. Since neat PES has negative charges on the surface, we prepared LbL assemblies of [PAH/PSS]₂ on the surface of PES membrane to construct PES/[PAH/PSS]₂ membranes [36,41]. Here, two [PAH/PSS] bilayers were deposited on the PES surface to provide a uniform surface charge. In this structure, negatively charged PSS layer was placed on the top surface of PES/[PAH/PSS]₂ membranes, which could facilitate electrostatic interaction with positively charged TiO₂ NPs. Therefore, we immersed PES/[PAH/PSS]₂ membranes in the aqueous solution of TiO₂ NPs for an extended period of time (1 week) to induce equilibrated NP deposition to the PSS layer on PES membrane. The uniform coating of TiO₂ NPs on the surface of PES membrane has been confirmed by plan-view (Figure 7a-7c) and cross-sectional (Figure 7d-7f) SEM images. By examining SEM images of Figure 7a and 27, one can find that round-shaped pores having hundreds nanometer diameters are distributed over the entire membrane by forming sponge-like structures. Here, it must be noted that PES polymer does not have practical solubility in water (solubility parameter of PES and water = $\sim 24.0 \text{ MPa}^{1/2}$ and $48.0 \text{ MPa}^{1/2}$) [42]. Hence, the membrane structures were not altered during the deposition of PAH, PSS, and TiO₂ NPs in the aqueous solutions. In addition, along with the enlarged SEM images, it can be validated that TiO₂ NPs

are uniformly coated on the top and inner surface of membranes without the formation of noticeable NP agglomeration. Since agglomeration of NPs can inhibit their photocatalytic activity, the uniform coating of NPs on PES membranes would exert better photocatalytic activity. For simplicity, PES membranes with [PAH/PSS]₂/TiO₂ NPs will be denoted as PES/TiO₂ membranes, hereafter.



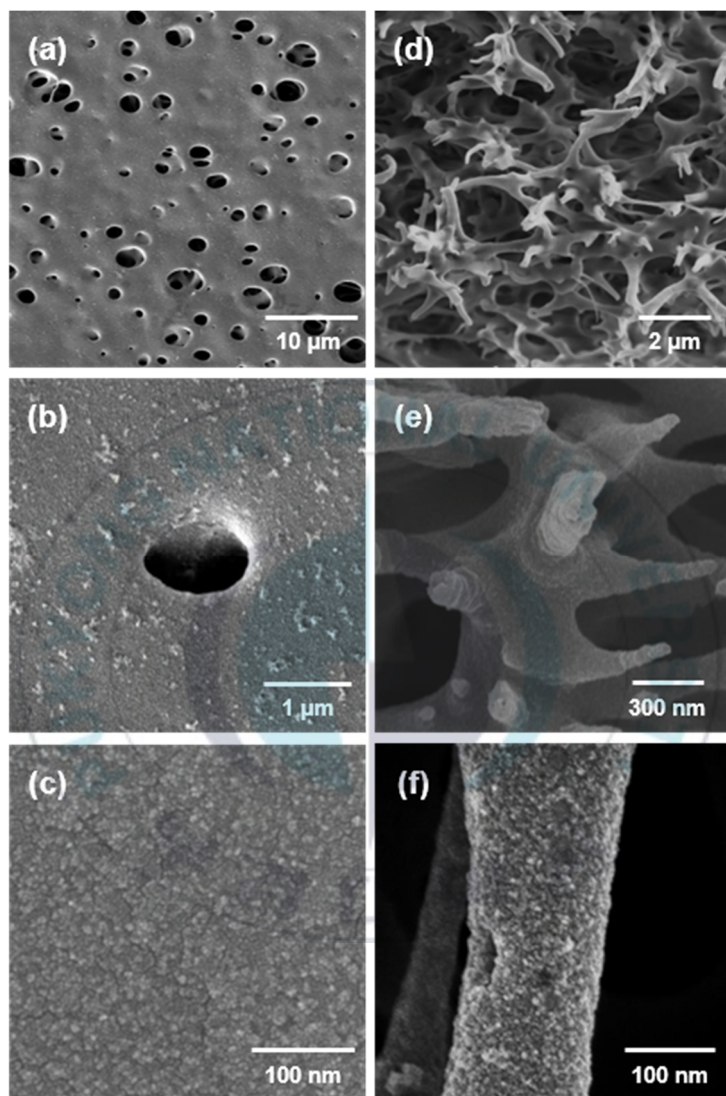


Figure 7. (a – c) Plan-view and (d – e) cross-sectional SEM images of PES membranes with $[PAH/PSS]_2/TiO_2$ NPs with different magnifications.

II-3.3. Enhanced Photocatalytic Activity of Immobilized TiO₂ Nanoparticles

Having analyzed the structures of PES/TiO₂ membrane, we applied the composite membranes to a model chemical reaction. In particular, photocatalytic decomposition of dye molecules was tested because dyes can represent the organic pollutants in aquatic ecosystem. For the purpose, the prepared PES/TiO₂ membrane (diameter = 25 mm) was placed into 15 mL of methylene blue (MB) under dark container and monitored the changes of absorption bands upon incubation. It needs to be noted that MB has two major absorption bands at 293 nm ($\pi - \pi^*$) and 664 nm ($n - \pi^*$) in dilute aqueous solution [43]. However, the absorption band at 293 nm strongly overlap with the absorption of TiO₂ NPs (Figure 6b). Therefore, we monitored the time-dependent absorption at 664 nm throughout this study. In the UV-Vis spectra of Figure 8a, the MB absorbance at 664 nm gradually decreased with time under dark condition. Since photocatalytic reaction of TiO₂ NPs cannot occur without UV light, the decreased MB absorbance can be attributed the electrostatic adsorption of cationic MB to the anionic PSS layer on PES/[PAH/PSS]₂ membranes. Consequently, the color of membrane was turned into bluish as shown in the inserted photo of Figure 8a. When the same photocatalytic reaction of PES/TiO₂ membrane was performed under identical condition but in the presence of external light source (by solar simulator), the decrease in the MB absorbance became much faster as shown in Figure 8b. Here, it needs to be noted that, in the absence of PES/TiO₂ membranes, the MB absorbance in the

aqueous solution was not altered under the same illumination (data not shown). Therefore, the decreased UV-Vis spectra in Figure 8b indicated photocatalytic decomposition of MB molecules by TiO₂ NPs in the composite membrane. Here, it needs to be noted that MB absorbance could be reduced not only by photocatalysis, but also by the electrostatic adsorption of MB molecules to the membrane. However, unlike dark condition, the photo-excited TiO₂ NPs in the composite membrane decomposed most of the adsorbed MB molecules, which was confirmed from the white color of the composite membrane after the photocatalytic reaction (see inserted photo of Figure 8b). Hence, the UV-Vis spectra in Figure 8b can be solely attributed to the photocatalytic decomposition of MB.

For a more quantitative analysis, the absorbance value at 664 nm during the time course of reaction was fitted by using a first-order kinetics equation of $\ln(C/C_0) = -kt$, at which C_0 and C are the concentration of MB molecules at initial and given time t , respectively, and k is the rate constant. From the fitted lines (Figure 8c), it can be validated that the rate of decomposition under light illumination (red color) was much faster than the rate of absorption under dark (black color). For each cases, the rate constants were evaluated from independent three measurements, and the average rate constant was evaluated as $2.12 \times 10^{-3} \text{ min}^{-1}$ under dark and $8.13 \times 10^{-3} \text{ min}^{-1}$ under illumination conditions.

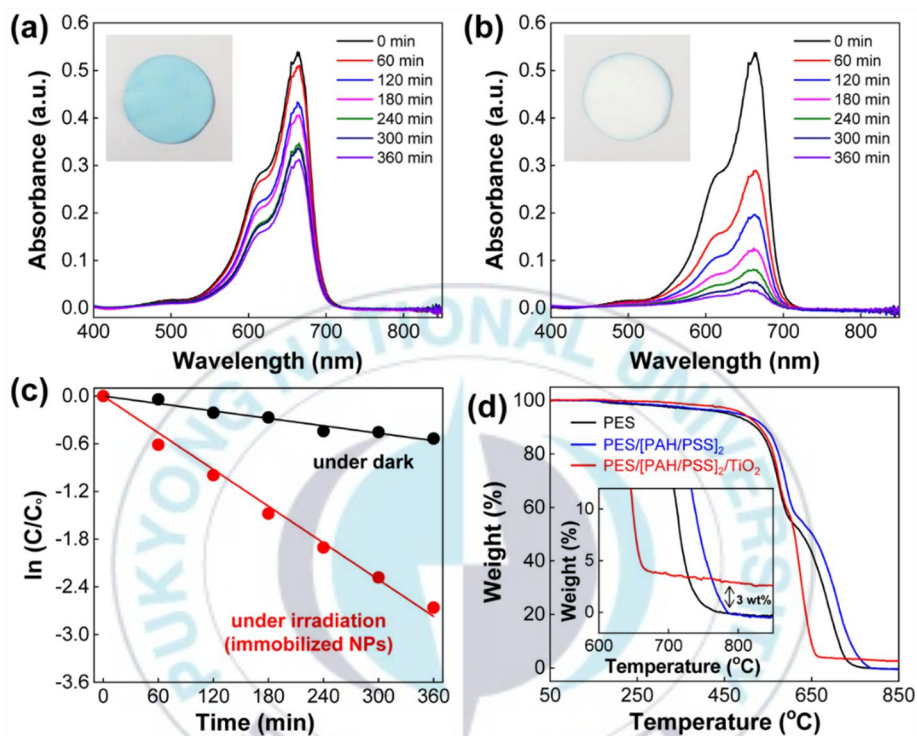


Figure 8. (a, b) Time-dependent UV-Vis spectra of photocatalytic decomposition of MB in the presence of PES/TiO₂ composite membrane without (a) and with (b) light illumination. (c) Time-dependent absorbance values at 664 nm in the time course of photocatalytic decomposition of MB with (red color) and without (blue color) light illumination. (d) TGA results of PES (black), PES/[PAH/PSS]₂ (blue), and PES/[PAH/PSS]₂/TiO₂ NPs under air environment.

Confirming the decomposition of MB molecules, we turned our attention to the photocatalytic efficiency of the immobilized TiO_2 NPs in comparison with the dispersed ones. In particular, we focused on the question whether the PES membranes could enhance or reduce the catalytic activity of immobilized NPs. To this end, we first evaluated the amount of TiO_2 NPs deposited on the PES membrane by thermogravimetric analysis (TGA). In this technique, since inorganic TiO_2 NPs are thermally stable without decomposition under air condition, the mass of immobilized TiO_2 NPs could be evaluated by comparing the thermographs. As shown in Figure 8d, TGA curves from all the membranes exhibited sharp weight loss above $\sim 500^\circ\text{C}$, which would be attributed to the decomposition of PES frame. Nevertheless, the residual weight from PES/[PAH/PSS] $_2$ / TiO_2 membrane (red line) was clearly higher than that from PES/[PAH/PSS] $_2$ membrane (blue line), which can be attributed to the presence of the immobilized TiO_2 NPs in the PES membrane. From three independent TGA measurements, the residual mass of TiO_2 NPs was determined as 3.0 wt% of the initial composite membranes, which corresponded to 0.6 mg.

By utilizing the same amount of TiO_2 NPs (0.6 mg), we tested photocatalytic activity of the dispersed TiO_2 NPs in a solution state. In this set of experiment, it needs to be noted that the illuminated area by external light must be identical for the immobilized and dispersed NPs. Therefore, cylindrical glass dish having the same diameter with PES membrane (25 mm) was prepared, onto which MB solution (15 mL) and 0.6 mg of TiO_2 NPs were added with the same MB concentration. Since the beam diameter of Xenon lamp (~ 27 mm) was slightly larger than 25 mm, the photocatalytic activity

of the immobilized and dispersed NPs can be compared under the same illumination condition. As in the previous cases, time-dependent UV-Vis spectra were collected under dark (Figure 9a) and light illumination (Figure 9b). By comparing the results, one can find the catalytic decomposition of MB molecules by the dispersed TiO₂ NPs under light illumination. The experimental results were again fitted by a first-order kinetics equation to extract the rate constant (Figure 9c). Interestingly, the average rate constant from dispersed NPs ($6.22 \times 10^{-3} \text{ min}^{-1}$) was slower than that from immobilized NPs ($8.13 \times 10^{-3} \text{ min}^{-1}$). In other word, the photocatalytic activity of the immobilized NPs was higher than that of dispersed ones, the result of which was represented as red (immobilized) and blue (dispersed) fitted lines in Figure 9d.

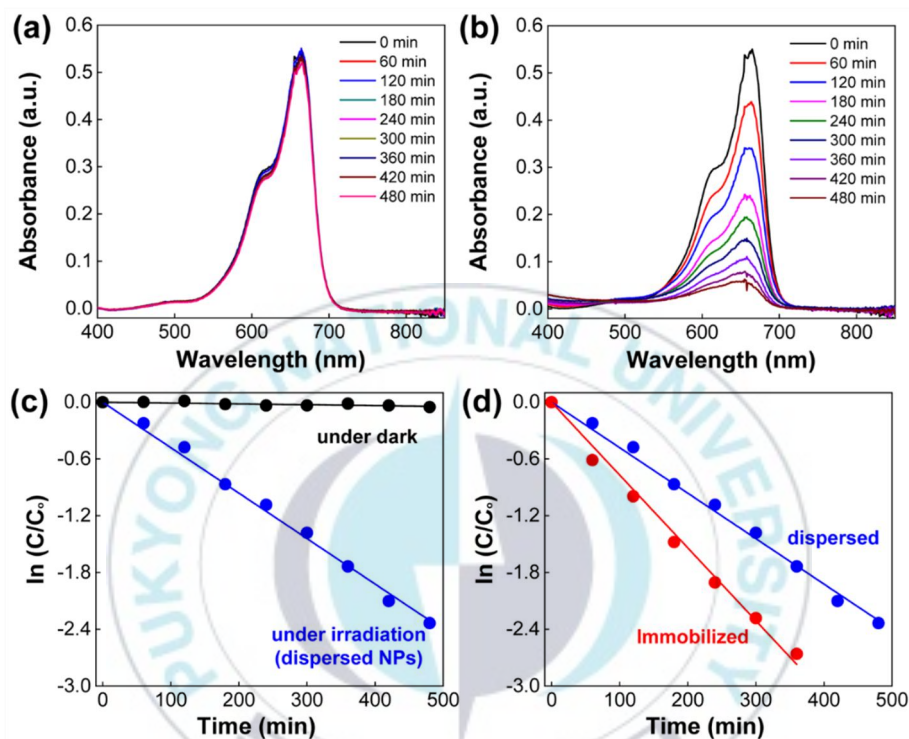


Figure 9. (a, b) Time-dependent UV-Vis spectra of MB photocatalytic decomposition in the presence of colloidal TiO₂ NPs without (a) and with (b) light illumination. (c) Time-dependent absorbance values at 664 nm in the time course of MB photocatalytic decomposition with (blue color) and without (blue color) light illumination. (d) Comparison of kinetics of MB decomposition from dispersed TiO₂ NPs (blue color) and immobilized TiO₂ NPs (red color).

II-3.4. Scattering-Mediated Absorption of PES/TiO₂ Composite Membranes

This observation would contradict to common expectation that dispersed NPs would have better catalytic performance than the immobilized ones because of their larger surface area as well as easier access to the reactants. To understand the unexpected photocatalytic performance from the immobilized NPs, we examined diffusely reflected lights from the composite membranes. As shown in Figure 10, neat PES membrane (blue line) exhibited very high reflectance (> 95%) at wavelength above 350 nm. Since PES polymer could not reflect any light in a dissolved state, the strong reflectance from PES membrane can be solely ascribed to the presence of porous structures. In particular, it has been reported that incident light can be strongly scattered and reflected at the interfaces of randomly oriented porous structures [8]. Similarly, PES/TiO₂ composite membrane (red line in Figure 10) also exhibited high reflectance. However, the intensity of the reflected light from the composite membrane was substantially reduced below ~400 nm in comparison with neat PES membrane. Since TiO₂ has bandgap in the UV region, the reduced reflectance from PES/TiO₂ membrane indicated that the scattered or reflected lights from the body of PES membrane was re-absorbed by the immobilized NPs. This indicated that the immobilized NPs in the composite membrane could be photo-excited not only by the external light source, but also by the scattered/reflected light within the membrane. As a result, the actual number of photons that can be absorbed by the immobilized

NPs would be enormously increased by the multiple scattering and reflectance events, which would result in the enhanced photo-catalytic activity in Figure 9d.

In this regard, it would be interesting to note that comparable scattering-mediated absorption process has been proposed as an efficient method to enhance light-absorbing ability of advanced colloidal photocatalytic systems [44-47]. For instance, Que et. al. synthesized flower-like TiO_2 microspheres, at which numerous nanoplates were attached on the surface of TiO_2 microspheres [44]. Owing to the multiple light reflection and scattering effects by the unique structures, TiO_2 microspheres exhibited improved light absorption and exhibited enhanced photocatalytic performance. In addition, flower-like $(\text{BiO})_2\text{CO}_3$ microspheres, mesoporous TiO_2 microbeads, and TiO_2 sphere-in-sphere colloids have been synthesized, which also took advantage of multiple scattering process to improve the absorption ability and the corresponding photocatalytic performance [45-47].

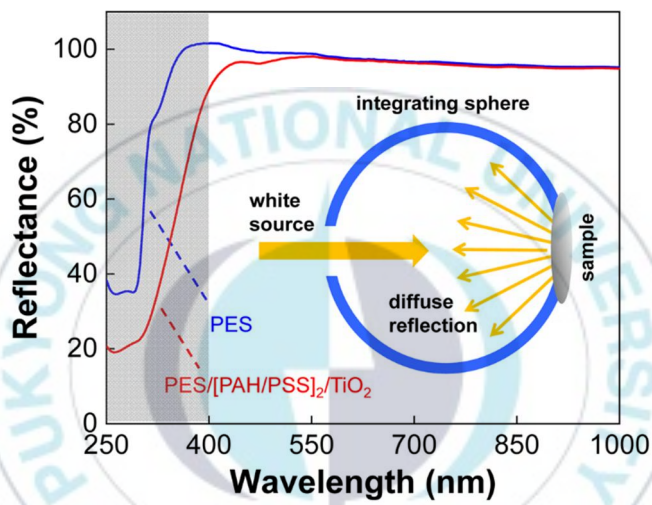


Figure 10. Diffuse reflectance of PES (blue) and PES/[PAH/PSS]₂/TiO₂ (red) membranes.

II-4. Conclusion

In this study, we prepared PES/[PAH/PSS]₂/TiO₂ composites by constructing LbL assembly on porous PES membranes to explore their photocatalytic property. By examining the kinetics of MB decomposition from the immobilized TiO₂ NPs in PES membrane, we discovered that photocatalytic performance of the immobilized NPs could be higher than that of dispersed ones. Light scattering and reflection in the composite membrane was suggested as the underlying principle for the enhanced photocatalysis from the perspectives that the optical path length of the incident light can be enormously increased by the multiple scattering process within the porous membrane. As a result, the immobilized NPs could have more chance to absorb the scattered light to enhance their photocatalytic performance. Overall, this research indicates that scattering-mediated absorption process in polymer-NP composites could have a potential to enhance the photocatalytic performance of existing semiconductor NPs.

Chapter III. Enhanced Photothermal Heating of Au Nanoparticles by Multiple Scattering Process in Composite Membranes for Heterogeneous Catalytic Reaction

III-1. Introduction

The utilization of solar energy to drive a chemical reaction is an emerging application of plasmonic nanoparticles (NPs). In this approach, the localized surface plasmon resonance (LSPR) of metal NPs, which is excited by solar radiation, can be transformed to light or local heat around NP surface depending on the decay process of excited LSPR. Since light and heat are important experimental parameters in chemistry, plasmonic NPs has been implanted into many chemical systems for practical applications in fluorescence, sensing, spectroscopy, and others [23,48-49]. Among others, plasmon-assisted catalytic reaction may represent the most efficient way of utilizing solar energy conversion because the equilibrium and kinetics of given catalytic reactions can be strongly regulated by the light and temperature. For instance, the photocatalytic TiO₂ NPs in water-splitting reaction could be strongly accelerated

by synthesizing Au@TiO₂ core-shell NPs, at which the absorption efficiency of TiO₂ shell was strongly enhanced by experiencing the local field produced by Au core [50]. In another example, the temperature of reaction medium can be increased by photothermal effect of metal NPs [9]. Since the rate constant of chemical reaction can be mostly described by Arrhenius equation of $k = A \exp(-E_a/RT)$, the change in temperature (T) substantially modify the kinetics of chemical reactions. At the same time, the high energy surface of metal NPs can work as catalytic sites to reduce activation energy (E_a) of given chemical reaction. From this perspective, one can convince that metal NPs can provide both plasmonic and catalytic functions to provide dual modality in chemical reactions.

Although plasmon-assisted catalysis holds a great promise in many chemical reactions, there is an inherent restriction in solar energy utilization owing to the limited spectral overlap in the system. Note, the representative plasmonic NPs such as Ag and Au have narrow extinction peaks in the visible region. Therefore, they can only interact with a certain portion of the solar radiation which overlaps with the LSPR peaks. In order to increase the degree of spectral overlap and to enhance the efficiency of solar energy conversion, the narrow LSPR peaks of metal NPs must be extended over broad range in the wavelength. In this standpoint, the superstructures of metal NPs, at which multiple NPs are assembled in the close vicinity of one another, have attracted a great deal of attention because LSPRs of individual NPs can be coupled together to shift the LSPR peaks to longer wavelength direction.

In this study, we introduced Au NPs inside porous polyethersulfone (PES) membrane by Layer-by-Layer (LbL) method. In the composite PES/Au membrane, Au NPs were homogeneously coated with a high density to induce extensive plasmonic coupling among NPs. As a result, the extinction of composite PES/Au membrane exhibited broadband absorption up to near-IR region, which allowed high degree of spectral overlap with solar radiation [24-25]. Since PES/Au composite membrane can harvest a large portion of solar energy, it can efficiently produce heat inside the membrane by plasmonic effect. We utilized the local heat, which is directly associated with the actual temperature during the chemical reaction, for the enhanced catalytic activity. In order to know the effect of presence or absence of photothermal effect, the catalytic reaction of 4-nitrophenol was carried out with or without light illumination.



Figure 11. Graphical abstract of immobilized Au NPs on the PES membrane surface, the composite membrane. In the formed composite membrane, Au NPs generate heat with illumination, and a polymer membrane scatters the incident light to the outside or inside. The internally scattered light induces multiple scattering process, which is absorbed by Au NPs or re-scattered by the surface of the assembly.

III-2. Experimental Section

III-2.1. Material

Polyethersulfone (PES) filtration membranes (diameter: 25 mm, pore size: 450 nm) were provided by Scilab Co., Korea. Poly(allylamine hydrochloride) (PAH, weight-average molecular weight = 17,500 g/mol), poly (sodium 4-styrenesulfonate) (PSS, 70,000 g/mol), gold (III) chloride trihydrate ($\text{HAuCl}_4 \cdot 3\text{H}_2\text{O}$, $\geq 99.9\%$), 4-nitrophenol (4-NP, $\geq 99\%$), sodium borohydride (NaBH_4 , 99 %) and sodium citrate tribasic dehydrate ($\geq 99\%$) were obtained from Sigma-Aldrich. All the chemicals were used as received.

III-2.2. Procedure

III-2.2.1. Synthesis of Colloidal Au

Au NPs were synthesized by citrate reduction method. 500 mL aqueous solution of $\text{HAuCl}_4 \cdot 3\text{H}_2\text{O}$ (0.5 mM) was simply heated until boiling, and 25 mL of sodium citrate solution (0.5 g in 25 mL) was added to the boiling solution. The mixture was further boiled for 15 min with vigorous stirring and then cooled to room temperature.

III-2.2.2. Synthesis of the PES/[PAH/PSS]_{1.5}/Au Composite Membrane

In order to apply layer-by-layer (LbL) assemblies, 1.0 wt% aqueous solution of

cationic polyelectrolyte by PAH and anionic polyelectrolyte by PSS were prepared. Basically, since the surface of the PES membrane has negative charge, the membrane was first immersed in an aqueous PAH solution for 3 h to deposit PAH which is a cationic polyelectrolyte [36,41]. Subsequently, PAH-coated PES membrane was alternatively immersed in an aqueous solution of anionic polyelectrolyte by PSS for 3hr, which produced PAH/PSS bilayer on the PES membrane. In between each coating step of PAH (or PSS) layer, the membrane was immersed in deionized water for 1 hr to remove physisorbed PAH (or PSS) polymers. The PES membrane with one bilayer of [PAH/PSS] was immersed once more into the aqueous PAH solution in order to be immobilized Au NPs having negative surface charge, the structure of PES/[PAH/PSS]/[PAH] will be denoted as PES/[PAH/PSS]_{1.5}. The chemically modified PES membrane was immersed in the colloidal Au for 3 days. Finally, the PES/[PAH/PSS]_{1.5}/Au NPs composite membrane was immersed in deionized water for 3 h.

III-2.2.3. Evaluation of Catalytic Reaction

In order for the catalytic effect to be evaluated, PES/[PAH/PSS]_{1.5}/Au NPs composite membranes were added into an aqueous mixture (15 mL) of 4-nitrophenol (2.67 μ M) and sodium borohydride (1.33 mM). The reaction mixture was placed either in dark container or illuminated by solar simulator. At a regular time interval, an aliquot of reaction mixture was taken to measure UV-Vis spectra. After measurement, the measured solution was poured back into the reaction mixture.

III-2.3. Measurement

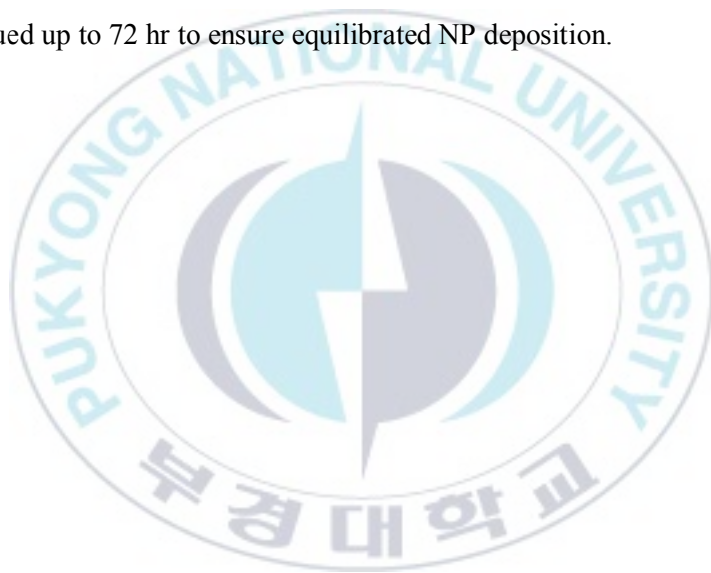
UV-Vis spectra were obtained using an Agilent Technologies Cary 8454 UV-Vis spectrophotometer. A high-resolution transmission electron micrograph (HR-TEM) was recorded by a JEOL JEM-2100F microscope, working with a 200 kV accelerating voltage. Field-emission scanning electron microscopy (FE-SEM) images were taken with a Hitachi High-Technologies S-4800. The catalytic experiments were performed under simulated solar light irradiation working with 1.0 sun at AM 1.5 G, using an Abet Technologies LS-150 equipped with an infrared cut-off filter. Diffuse reflectance of the membranes was recorded on a Shimadzu SolidSpec-3700 UV-Vis-NIR spectrophotometer. The thermal images were recorded by a Testo-868 thermal imaging camera.

III-3. Result and Discussion

III-3.1. Synthesis and Structural Properties of the Composite Membrane

In order to deposit Au NPs inside the PES membrane, we alternatively deposit polyelectrolytes of PAH and PSS on the negatively-charged PES to construct LbL assemblies of [PAH/PSS]_{1.5} on PES membranes (see Experimental section for the details). In this structure, since the topmost layer of the prepared PES/[PAH/PSS]_{1.5} membrane was composed of positively charged PAH, citrate-stabilized Au NPs having negative charges can be coated on the membrane surface by electrostatic

interaction. In this regard, we immersed PES/[PAH/PSS]_{1.5} membrane in the aqueous solution of Au NPs (average diameter = 12 nm) and measured the extinction spectra of NPs solution under different immersing time. As shown in Figure 12a, Au NP exhibited well-known LSPR peak at 520 nm. Initially, the extinction intensity was set as 1.0. After immersion, the peak intensity was monotonically decreased, indicating the depletion of Au NPs in the solution state. Note, the decrease of extinction peak was typically saturated after 36 hr (see inset of Figure 12a). Hence, the immersion was continued up to 72 hr to ensure equilibrated NP deposition.



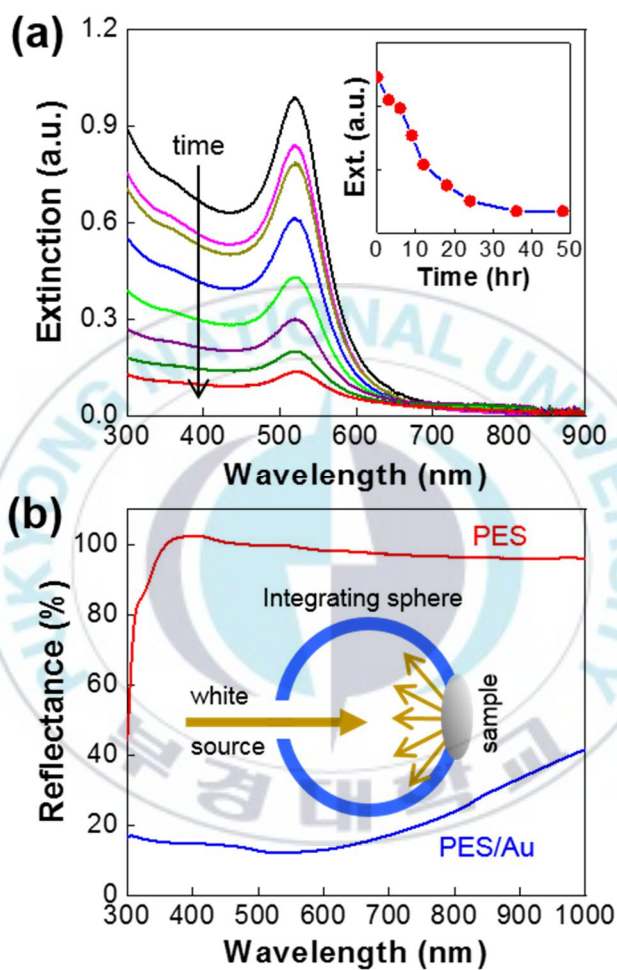


Figure 12. (a) Time-dependent of extinction spectra of Au NPs after the immersion of PES membrane. (b) Reflectance spectra of PES (red line) and PES/Au membranes (blue).

The uniform coating of NPs on the surface of PES/[PAH/PSS]_{1.5} membrane has been confirmed by FE-SEM analysis. As shown in the plan-view (Figure 13a, 13b) and cross-sectional (Figure 13c, 13d) SEM images, PES membranes have round-shaped pores having hundreds nanometer of diameters, which are interconnected with each other to form sponge-like structures in the cross sections. In the magnified images, one can find that Au NPs were densely coated on the membrane surface without noticeable NP agglomerations. Based on the structure, PES/[PAH/PSS]_{1.5}/Au NPs will be simply denoted as PES/Au composite membrane, hereafter. Interestingly, the color of PES membranes was turned into dark violet after the coating process (inset Figure 13a). Since the color of isolated Au NPs in a solution state was red, the dark appearance of PES/Au composite membranes indicated the presence of extensive plasmonic coupling among NPs. This eventually induced broadband absorption of coupled NPs up to near IR region (Figure 12b).

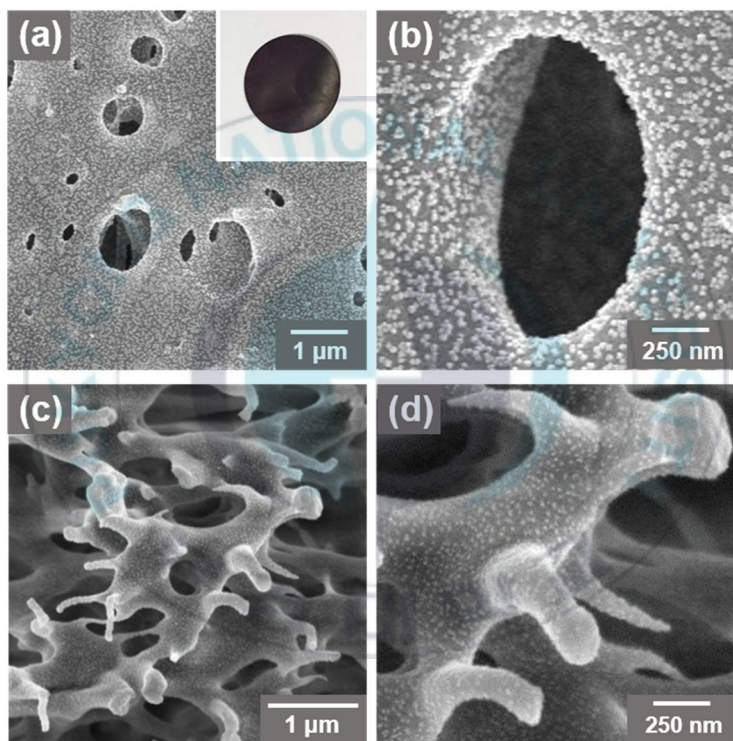


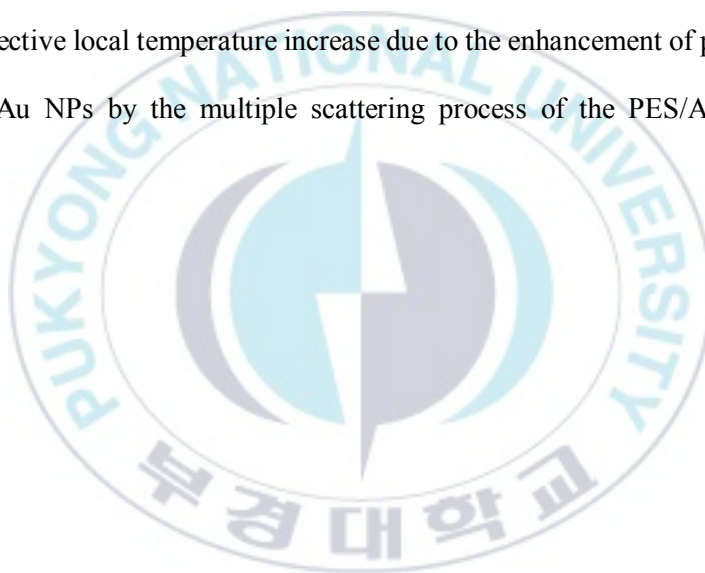
Figure 13. Plane-view (a, b) and cross-sectional (c, d) FE-SEM images of PES/Au composite membranes under different magnifications.

III-3.2. Catalytic Performance of the Composite Membrane

Having verified the structure and extinction of PES/Au composite membranes we testified their catalytic function. In particular, the reduction of 4-nitrophenol to 4-aminophenol with excess of NaBH_4 was selected as a model reaction because it can be easily monitored by UV–Vis spectroscopy. It needs to be noted that 4-nitrophenol solution shows a light-yellow color with a strong absorbance peak at 317 nm. On adding excess NaBH_4 , 4-nitrophenolate anions become the dominant species and the solution color changes to dark yellow with a red-shifted absorption peak to 400 nm (Figure 14a, 14b). However, the reduction of 4-nitrophenolate anions is kinetically restricted by the high activation energy, and only occurs in the presence of catalyst. Owing to these features, the reduction of 4-nitrophenol becomes one of the model reactions for evaluating the catalytic properties of many metal NP systems [51].

In our experiments, a 15 mL aqueous mixed solution containing 4-nitrophenol (4-NP) and sodium borohydride (SBH) having a concentration of 500 times of 4-NP was placed in the glass petri dish with a diameter of 50 mm. The catalytic reaction proceeded when a PES/Au composite membrane was immersed therein (Figure 14a, 14b). The UV-Vis peak reduction of 4-nitrophenolate at 400 nm was observed either under dark container (Figure 14a) or illuminated by solar simulator (Figure 14b). The absorbance value at 400 nm during the time course of reaction was fitted by using a first-order kinetics equation of $\ln(C/C_0) = -kt$, at which C_0 and C are the

concentration of 4-nitrophenolate anions at initial and given time t , respectively, and k is the rate constant. In Figure 14c (fitted lines from Figure 14a, 14b), the rate of the catalytic reaction under light irradiation (red line) was found to be much faster than under dark container (blue line). In order to observe for its tendency, the average values of reaction rate were evaluated as $3.36 \times 10^{-3} \text{ min}^{-1}$ under dark condition (k) and $6.30 \times 10^{-3} \text{ min}^{-1}$ under light illumination (k') (Table 1). Briefly, the cause of the enhanced catalytic performance under light irradiation could be expected to be an effective local temperature increase due to the enhancement of photothermal effects of Au NPs by the multiple scattering process of the PES/Au composite membrane.



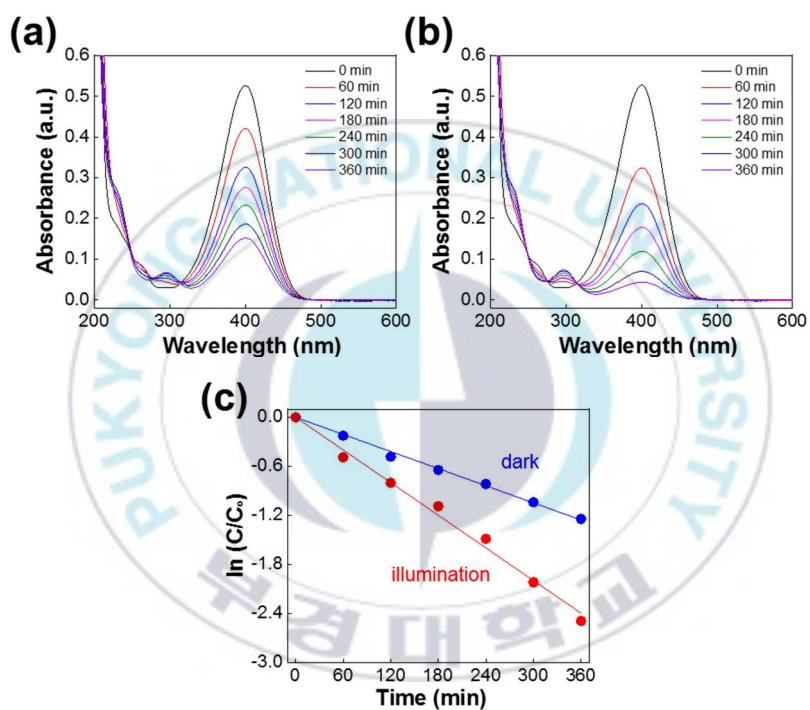
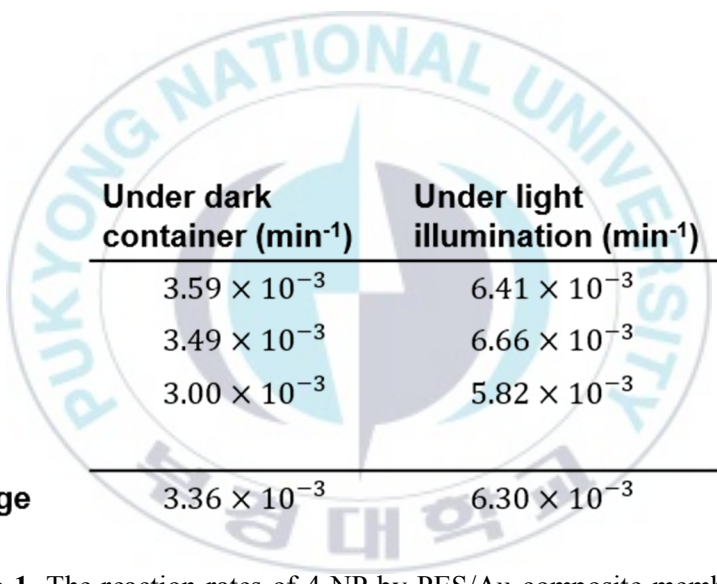


Figure 14. (a, b) Time-dependent UV-Vis spectra of catalytic reaction of 4-NP in the presence of the PES/Au composite membrane under dark condition (a) and under light illumination (b). (c) Time-dependent absorbance values at 400 nm in the time course of 4-NP catalytic reaction under dark container (blue line) and under light illumination (red line).



| Trial | Under dark container (min ⁻¹) | Under light illumination (min ⁻¹) | Ratio (k ['] /k) |
|----------------|--|--|------------------------------|
| 1 | 3.59×10^{-3} | 6.41×10^{-3} | 1.786 |
| 2 | 3.49×10^{-3} | 6.66×10^{-3} | 1.908 |
| 3 | 3.00×10^{-3} | 5.82×10^{-3} | 1.940 |
| Average | 3.36×10^{-3} | 6.30×10^{-3} | 1.878 |

Table 1. The reaction rates of 4-NP by PES/Au composite membranes were repeated three times independently for each trial.

III-3.3. Evaluation of Local Temperature by the Composite Membrane

In order to demonstrate the heat generating effect of the PES/Au composite membrane with light illumination, the activation energy (E_a) for 4-NP catalytic reaction was calculated at four different temperatures (Figure 15a). Basically, the activation energy can be measured through the Arrhenius equation of $k = A \exp(-E_a/RT)$, the change in temperature (T) substantially modify the kinetics of chemical reactions. Temperature-dependent reaction rates (k) were measured as $5.35 \times 10^{-3} \text{ min}^{-1}$ at 23.1°C (black color), $8.26 \times 10^{-3} \text{ min}^{-1}$ at 30.6°C (red color), $1.26 \times 10^{-2} \text{ min}^{-1}$ at 39.5°C (blue color), and $1.60 \times 10^{-2} \text{ min}^{-1}$ at 51.8°C (green color) through temperature control using oil baths (Figure 15a). Then, Arrhenius equation gives a straight-line plot ($y = mx + b$) for $\ln k$ versus $1/T$ (Figure 15b). From Figure 15b, the slope of the straight line is $-\frac{E_a}{R}$, through which its E_a value is obtained as $3.06 \times 10^4 \text{ J/mol}$. By applying this E_a value, the local temperature increase effect from Figure 14 is able to be calculated through the ratio of reaction rates ($\frac{k'}{k}$). Note, k' is the rate of 4-NP catalytic reaction under light illumination and k is the rate of 4-NP catalytic reaction under dark container. The average value of the repeated measured ratios is 1.878 (Table 1), and the local temperature increase effect is calculated as $+15.5^\circ\text{C}$ through another form of

Arrhenius equation : $\ln\left(\frac{k}{k_0}\right) = \frac{E_a}{R} \left(\frac{1}{T} - \frac{1}{T_0}\right)$. These results are very interesting because the PES/Au composite membrane causes the high level of local temperature increase under only light irradiation with IR cut-off filter. In particular, this evaluation reliably supports expectation from multiple scattering process by the PES membrane and broadband absorption by coupled Au NPs of the PES/Au composite membrane.



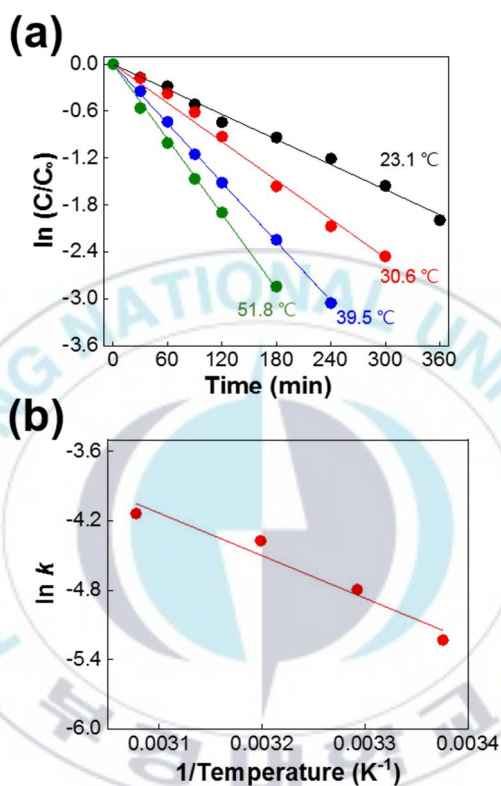
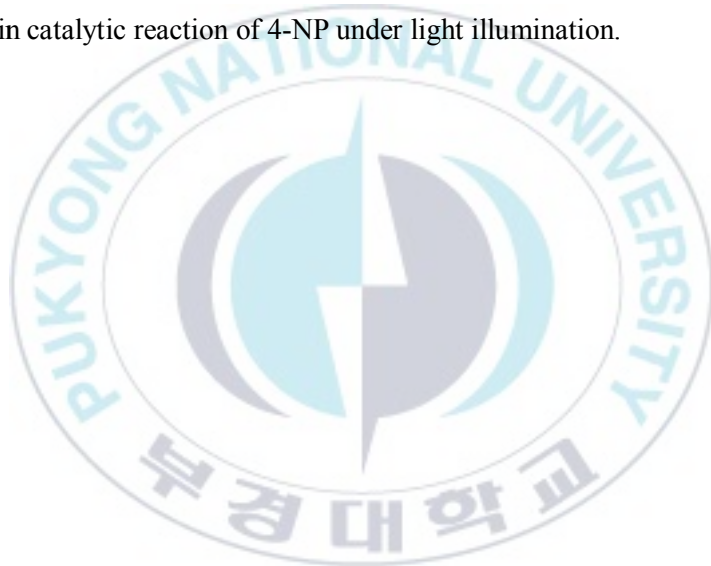


Figure 15. (a, b) Time-dependent UV-Vis spectra of catalytic reaction of 4-NP in the presence of PES/Au composite membranes at four different temperature conditions. (a) Time-dependent absorbance values at 400 nm in the time course of 4-NP catalytic reaction under 23.1 °C (black line), 30.6 °C (red line), 39.5 °C (blue line) and 51.8 °C (green line), respectively. (b) $\ln k$ versus $1/T$ of the straight line. The activation energy (E_a) can be calculated through its slope ($-\frac{E_a}{R}$).

III-3.4. Combination of Multiple Scattering Process and Broadband Absorption

This observation would present some interesting points about coupled Au NPs on the polymer membranes. In order to smoothly illustrate such views, it is necessary to be clear about the role of Au NPs and polymer membranes. As shown in Figure 13, immobilized and coupled Au NPs on the PES/[PAH/PSS]_{1.5} membrane could be visually confirmed by FE-SEM analysis. In Figure 12b, broadband absorption of the PES/Au composite membrane would be analyzed as the coupling of immobilized Au NPs on the PES membrane. Obviously, the catalytic performance under light illumination provided sufficient support for these empirical analyzes. In addition, the temperature of the reactor was observed using a thermal imaging camera (Figure 16a-c). In the temperature measurement of the reactor via a thermal imaging camera, the average temperature increase of 10.6 °C under light illumination (Figure 16b) was found compared with dark container (Figure 16c). Interestingly, it makes the high local temperature increase (15.5 °C) meaningful. In other words, there is a temperature difference between the temperature of the reactor and the surface of PES/Au composite membranes, which is the surface where the catalytic reaction actually progresses. Despite being immersed in the aqueous solution, the PES/Au composite membrane was constantly generating heat with illumination to stably

sustain its combined effect of multiple scattering properties and the broadband absorption. Also, Figure 16d shows the irradiance spectra of used solar simulator with IR cutting-off (green line), absorption spectra of colloidal Au (red line) and immobilized Au NPs on the PES membrane (blue line). In particular, absorption spectra of the PES/Au composite membrane (Figure 14d, blue line) is an excellent evidence of broadband absorption compared with the colloidal Au (Figure 14d, red line). They would cause strong local temperature increase of the PES/Au composite membrane in catalytic reaction of 4-NP under light illumination.



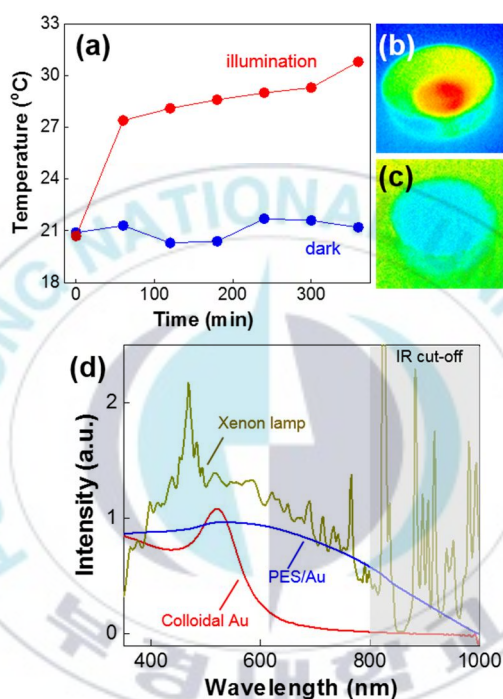


Figure 16. (a) Time-dependent temperature measurement in the 4-NP catalytic experiment of PES/Au composite membranes under dark container (blue line) and light illumination (red line). Images of the reactor taken with a thermal imaging camera after 360 min of catalytic experiments start under light illumination (b) and dark container (c). (d) Irradiance spectra of the solar simulator (green line), absorption spectra of colloidal Au (red line) and the PES/Au composite membrane (blue line).

III-4. Conclusion

In this study, we prepared polymer-nanoparticles composite membranes by controlling charge on surface of the porous PES membrane through LbL assembly for being immobilized Au NPs. The catalytic performance of the prepared composites was mainly evaluated and described the evidence that caused. First of all, broadband absorption was explained through reflectance spectra of PES/Au and demonstrated enhanced light absorption properties of immobilized Au NPs, which was coupled onto the PES membrane surface. Obviously, it caused better catalytic performance of the composite under light illumination. In addition, the local temperature effect through activation energy was calculated quantify the heat generating properties of the composite. Moreover, heat generating properties were compared to the reactor temperature through a thermal imaging camera, and interestingly it was found that the local temperature effect strongly existed. As a result, when the incident light reaches the surface of the composite, it undergoes multiple scattering processes by the polymer membrane. Consequently, they combine with broadband absorption properties of coupled Au NPs to create local temperature effects.

References

- [1] M. Ulbricht (2006), *Polymer*, **47**, 2217.
- [2] P. M. Budd, K. J. Msayib, C. E. Tattershall, B. S. Ghanem, K. J. Reynolds, N. B. Mckeown, and Detlev Fritsch (2005), *Journal of Membrane Science*, **251**, 263.
- [3] M. T. Ravanchi, Tahereh Kaghazchi, and A. Kargari (2006), *Desalination*, **235**, 199.
- [4] M. Padaki, R. S. Murali, M.S. Abdullah, N. Misdan, A. Moslehyani, M.A. Kassim, N. Hilal, and A.F. Ismail (2014), *Desalination*, **357**, 197.
- [5] A. Rahimpour, S.S. Madaeni, A.H. Taheri, and Y. Mansourpanah (2008), *Journal of Membrane Science*, **313**, 158.
- [6] J. Lee, H. R. Chae, Y. J. Won, K. Lee, C. H. Lee, H. H. Lee, I. C. Kim, and J. Lee (2013), *Journal of Membrane Science*, **448**, 223.
- [7] J. Zhang, Z. Xu, W. Mai, C. Min, B. Zhou, M. Shan, Y. Li, C. Yang, Z. Wang, and X. Qian (2013), *Journal of Materials Chemistry A*, **1**, 3101.
- [8] L. Yang, Q. Zhai, G. Li, H. Jiang, L. Han, J. Wang, and E. Wang (2013), *Chemical Communication*, **49**, 11415.

- [9] S. H. Jo, H. W. Kim, M. Song, N. J. Je, S. Oh, B. Y. Chang, J. Yoon, J. H. Kim, B. Chung, and S. I. Yoo (2015), *ACS Applied Materials & Interfaces*, **7**, 18778.
- [10] M. Yang, T. Chen, W. S. Lau, Y. Wang, Q. Tang, Y. Yang, and H. Chen (2009), *small*, **5**, 198.
- [11] S. Y. Lee, and S. J. Park (2013), *Journal of Industrial and Engineering Chemistry*, **19**, 1761.
- [12] M. N. Chong, B. Jin, C. W. K. Chow, and C. Saint (2010), *Water Research*, **44**, 2997.
- [13] A. L. Linsebigler, G. Lu, and J. T. Yates, and Jr. (1995), *Chemical Reviews*, **95**, 735.
- [14] E. Bet-moushoul, Y. Mansourpanah, Kh. Farhadi, and M. Tabatabaei (2016), *Chemical Engineering Journal*, **283**, 29.
- [15] M. M. Pendergast, and E. M.V. Hoek (2011), *Energy & Environmental Science*, **4**, 1946.
- [16] N. Xu, Z. Shi, Y. Fan, J. Dong, J. Shi, and M. Z. C. Hu (1999), *Industrial & Engineering Chemistry Research*, **38**, 373.
- [17] C. Chen, R. Hu, K. Mai, Z. Ren, H. Wang, G. Qian, and Z. Wang (2011), *Crystal Growth & Design*, **11**, 5221.
- [18] M.A. Barakat, H. Schaeffer, G. Hayes, and S. Ismat-Shah (2005), *Applied Catalysis B: Environmental*, **57**, 23.
- [19] A. W. Xu, Y. Gao, and H. Q. Liu (2002), *Journal of Catalysis*, **207**, 151.

- [20] V. Subramanian, E. E. Wolf, and P. V. Kamat (2003), *Langmuir*, **19**, 469.
- [21] K. M. Mayer, and J. H. Hafner (2011), *Chemical Reviews*, **111**, 3828.
- [22] L. Dykman, and N. Khlebtsov (2011), *Chemical Society Reviews*, **41**, 2256.
- [23] I. H. El-Sayed, X. Huang, and M. A. El-Sayed (2005), *Nano Letters*, **5**, 5, 829.
- [24] T. Søndergaard, S. M. Novikov, T. Holmgaard, R. L. Eriksen, J. Beermann, Z. Han, and S. I. Bozhevolnyi (2012), *Nature Communications*, **3**.
- [25] K. Bae, G. Kang, S. K. Cho, W. Park, and K. Kim (2015), *Nature Communications*, **6**.
- [26] S. K. Loeb, P. J. J. Alvarez, J. A. Brame, E. L. Cates, W. Choi, J. Crittenden, D. D. Dionysiou, Q. Li, G. Li-Puma, X. Quan, D. L. Sedlak, T. D. Waite, P. Westerhoff, and J. H. Kim (2019), *Environmental Science & Technology*, **53**, 2937.
- [27] M. R. Hoffmann, S. T. Martin, W. Choi, and D. W. Bahnemann (1995), *Chemical Reviews*, **95**, 69.
- [28] A. Fujishima, X. Zhang, and D. A. Tryk (2008), *Surface Science Reports*, **63**, 515.
- [29] D. L. Liao, and B. Q. Liao (2007), *Journal of Photochemistry and Photobiology A*, **187**, 363.
- [30] M. H. Priya, and G. Madras (2006), *Journal of Photochemistry and Photobiology A*, **178**, 1.

- [31] G. Sivalingam, K. Nagaveni, M. S. Hegde, and G. Madras (2003), *Applied Catalysis B*, **45**, 23.
- [32] W. Choi, A. Termin, and M. R. Hoffman (1994), *The Journal of Physical Chemistry*, **98**, 13669.
- [33] Y. Gao, M. Hu, and B. Mi (2014), *Journal of Membrane Science*, **455**, 349.
- [34] G. R. Meseck, R. Kontic, G. R. Patzke, and S. Seeger (2012), *Advanced Functional Materials*, **22**, 4433.
- [35] D. N. Priya, J. M. Modak, and A. M. Raichur (2009), *ACS Applied Materials & Interfaces*, **1**, 2684.
- [36] P. Kaner, D. J. Johnson, E. Seker, N. Hilal, and S. A. Altinkaya (2015), *Journal of Membrane Science*, **493**, 807.
- [37] S. Mozia, D. Darowna, A. Orecki, R. Wróbel, K. Wilpiszewska, and A. W. Morawski (2014), *Journal of Membrane Science*, **470**, 356.
- [38] R. A. Damodar, S.-J. You, and H.-H. Chou (2009), *J. Hazard. Mater.*, **172**, 1321.
- [39] S. H. Kim, S.-Y. Kwak, B.-H. Sohn, and T. H. Park (2003), *Journal of Hazardous Materials*, **211**, 157.
- [40] G. Kang, and Y. Cao (2012), *Water Research*, **46**, 584.
- [41] L. Ricq, A. Pierre, S. Bayle, and J.-C. Reggiani (1997), *Desalination*, **109**, 253.
- [42] G. Wypych, *Handbook of Polymers*, ChemTec Publishing, 2d edn, 2016.

- [43] D. Heger, J. Jirkovský, and P. Klán (2005), *The Journal of Physical Chemistry A*, **109**, 6702.
- [44] Z. He, and W. Que (2013), *Physical Chemistry Chemical Physics*, **15**, 16768.
- [45] T. Xiong, F. Dong, and Z. Wu (2014), *RSC Advances*, **4**, 56307.
- [46] Z. Zheng, B. Huang, X. Qin, X. Zhang, and Y. Dai (2010), *Chemistry – A European Journal*, **16**, 11266.
- [47] H. Li, Z. Bian, J. Zhu, D. Zhang, G. Li, Y. Huo, H. Li, and Y. Lu (2007), *Journal of the American Chemical Society*, **129**, 8406.
- [48] P. K. Jain, X. Huang, I. H. El-Sayed, and M. A. El-Sayed (2007), *Plasmonics*, **2**, 107.
- [49] N. G. Khlebtsov, and L. A. Dykman (2010), *Journal of Quantitative Spectroscopy & Radiative Transfer*, **111**, 1.
- [50] H. Li, Z. Bian, J. Zhu, Y. Huo, H. Li, and Y. Lu (2007), *Journal of the American Chemical Society*, **129**, **15**, 4538.
- [51] S. Wunder, F. Polzer, Y. Lu, Y. Mei, and M. Ballauff (2010), *The Journal of Physical Chemistry C*, **114**, **19**, 8814.

Acknowledgements

First, I give my gratitude to my mentor and advisor, Professor Seong Il Yoo. From you, I got countless help from undergraduate to graduate school. Next, I would like to thank my family for their support and love. I think that I've done well because you are with me all day. Obviously, you have made me hard and diligent for a couple of years. Also, I express my special gratitude to Yoo's group members, which are Maulida Zakia, Limpat Nulandaya, Ja Min Koo, Merreta Noorenza Biutty and Geon Seok Lee. I do not doubt that the time we have together has become our deep friendship and memories.

Pukyong National University, Busan, South Korea

June 2019

Chang Hyeon Song